CONTEXTUALIZING RADON ACTIVITY IN NORTHEASTERN IOWA CAVES BY MEASURING URANIUM AND THORIUM AT THE RADON SAMPLING SITES

Lawrence E. Welch*, Brian E. Paul, Anna Takashima, Garrett D. Rau, Christopher L. Beck, Edward C. Klausner, Elizabeth R. Miller, Mark D. Jones, and Michael J. Lace

Knox College
Galesburg, Illinois, USA
lwelch@knox.edu

Abstract

A selection of caves in northeastern Iowa from similar geological strata were chosen as sampling sites for radon. At the radon measurement locations, physical samples were collected from the caves, and elemental analyses for uranium and thorium were performed. Collected materials included pieces of bedrock, soil, water and speleothems, all found in direct proximity to the radon sampling locations. An analysis of the amalgamated results was then made to seek out linkages between metal concentrations, radon activity, and cave structure.

(1) The authors have received partial funding from Knox College to support the research leading to this publication, including allocations from the Billy Geer Fund, the Andrew W. Mellon Foundation, the Committee On Faculty Research, and the Paul K. and Evalyn Elizabeth Cook Richter Trusts.

Introduction

The most common radon isotopes are all produced as a step in a decay series originating from either uranium or thorium (Cothern, 1987): ^{222}Rn is produced by the ^{238}U decay series and ^{220}Rn from the ^{232}Th decay series. On average, the earth's crust contains 2.7 ppm of uranium and 9.6 ppm of thorium (Rumble, 2018). Radon levels correlate with the concentration of the source elements in the surroundings only at the two extremes of concentration (Cothern, 1987). Hawaii has the lowest average indoor radon concentration of any state, which is attributable to extremely low uranium levels in the bedrock that makes up the island chain (Reimer, 2005). On the other hand, some uranium mines have shown stupendous levels of radon (Fijałkowska-Lichma, 2016), as might be expected. In the middle concentration ranges, the importance of factors impacting the transport and trapping of radon make the environmental uranium concentration not necessarily an ironclad predictor of radon activity.

A series of recent studies has measured radon levels in northeastern Iowa caves, finding some very high values. (Welch, 2015-2019). These caves are formed in limestone bedrock, which is primarily $CaCO_3$ from a chemical perspective. However, impurities are present in the limestone, with magnesium being the most prevalent, but many other metal impurities are present at trace levels. Most sources refer to limestone in general as low in uranium and thorium content. Ayotte et al., working in the Northern United States, found a typical uranium concentration of 2 ppm in limestone (Ayotte, 2007). Guilinger and Theobald found some limestone containing a significant amount of uranium in central Wyoming, but they felt that this uranium was due to secondary deposits from uranium-rich waters interacting with the original limestone (Guilinger, 1957). Kamaluddin and Amin, looking at multiple samples from Malaysia, found that most limestones contained less than 2 ppm of both uranium and thorium, although each set contained an outlier that was more than double the amount of each element in all the other samples (Kamaluddin, 1992). Zhao and Zheng evaluated many limestone samples from South China, and found almost all of them to have less than 1 ppm of both uranium and thorium (Zhao, 2014). El-Taher and Abdelhalim, using neutron activation analysis to evaluate limestone from Egypt, found an average uranium level of 2.7 ppm, and thorium of 9.6 ppm (El-Taher, 2014), coincidentally matching the values for the earth's crust cited earlier (Rumble, 2018).

Description of the Study Caves

Three different northeastern Iowa caves were selected for study, whereby in-cave locations were identified for radon measurements and then proximate physical samples were removed for uranium/thorium elemental analysis. All three caves are in the same general carbonate strata, the limestone and dolomite (dolomite is a close analog of limestone, where a significant portion of the calcium has been replaced by magnesium) of the Galena Group of the Ordovician Period, so would be expected to be more similar than not in terms of bedrock composition as a result (Lace, 2021). Figure (1) shows the locations of the three study caves within an Iowa state map. Figure (2) is a photograph taken near one of the sampling locations used in this study. The cave bedrock is an obvious element of the passage, yet sediment deposits and water from the cave

stream are present as well. As the sediment and water make up a significant fraction of the passage cross-section, they were also of interest as potential radon sources. A smaller element in

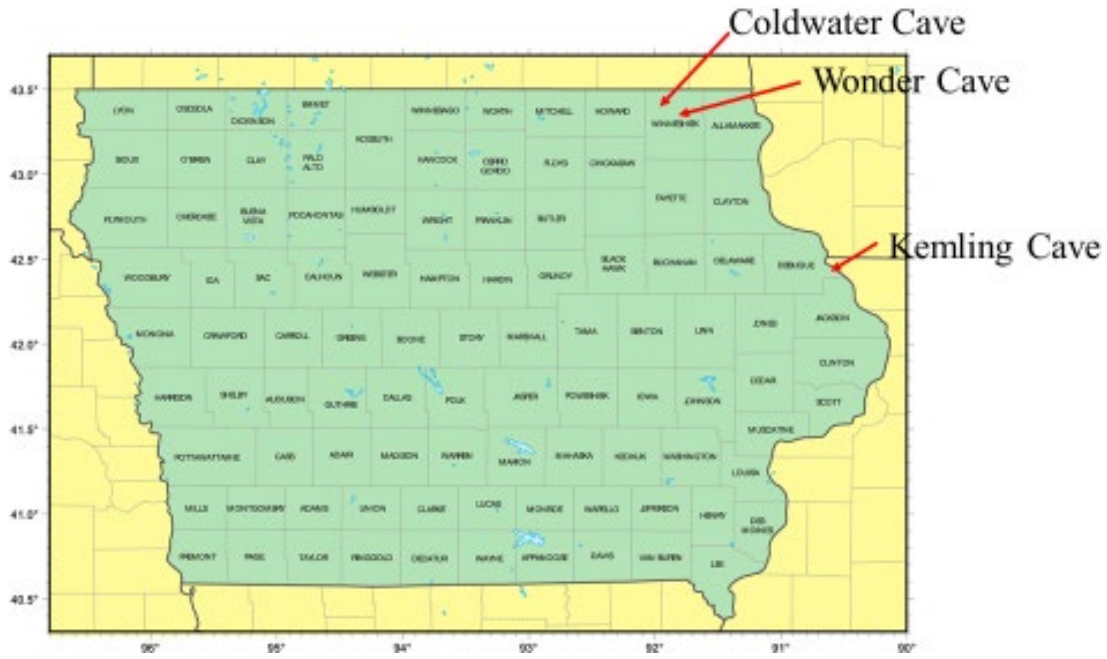

Figure (1): Locations of study caves.

Figure (2): Typical passage cross section, Coldwater Cave, near Station 5. Photo courtesy of www.scottdankofphoto.com.

Figure (2), but more significant in other cave locations, are speleothems or cave formations, which are secondary mineral deposits in the cave (Palmer, 2007). Most of the speleothems encountered in northeastern Iowa limestone caves are made via calcite (a specific crystal structure of $CaCO_3$) deposition under epigenic conditions (Palmer, 2007). In this process, normally water-insoluble limestone is dissolved by acidified water draining in from the surface. The bulk of the acidification is from passing through the soil, with its high concentration of CO_2 as a biomass waste product, which reacts in water to produce carbonic acid (H_2CO_3). The acidic water then dissolves the limestone to form Ca^{2+} and HCO_3^-. If the water containing these ions reaches airspace that has low airborne CO_2, this will lead to a shift in the chemical equilibrium, where the carbonic acid is consumed and the product of the process is CO_2, which is outgassed into the airspace. This process reduces the solution acidity, which also reduces the solubility of $CaCO_3$, which ultimately becomes supersaturated and then is precipitated as the calcite speleothem. When speleothems were present at the radon sampling location, it was desirable to do elemental analysis for the speleothems in addition to the bedrock, sediment, and water, if permission could be obtained. Since speleothems are a limited and fragile resource, only already-broken pieces were collected from the floor of the sampling sites to avoid breaking off a "living" formation.

Coldwater Cave is the first of the study caves; see Figure (3). It is essentially an underground river system found deep below the surface which has been surveyed to a length of 27.5 km with depths exceeding 30 meters. Coldwater can be classified as a zero entrance cave. This sounds

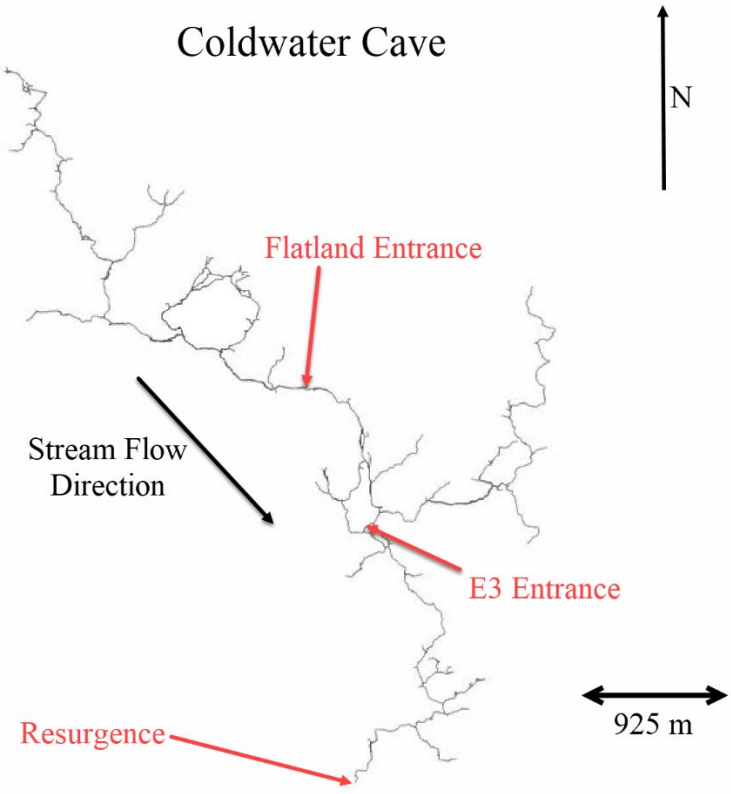

Figure (3): Plan view map of Coldwater Cave

nonsensical at first, but none of the three humanly-passable entrances permit significant air exchange with the outside environment. The natural resurgence of the cave river reaches a sump at its downstream extent, where water fills the passage to the ceiling for most of the last 400 meters of passage. The other two entrances (Flatland Entrance and E3 on Figure (3)) are drilled shafts that are kept hermetically sealed when not in use, which is only a small fraction of time.

Only a very small amount of gaseous communication exists with the outside environment, confirmed by the measurement of CO_2 levels in the cave and the dearth of bats seen in the cave over 30+ years of observation. Figure (4) shows a zoom of the Flatland entrance area showing

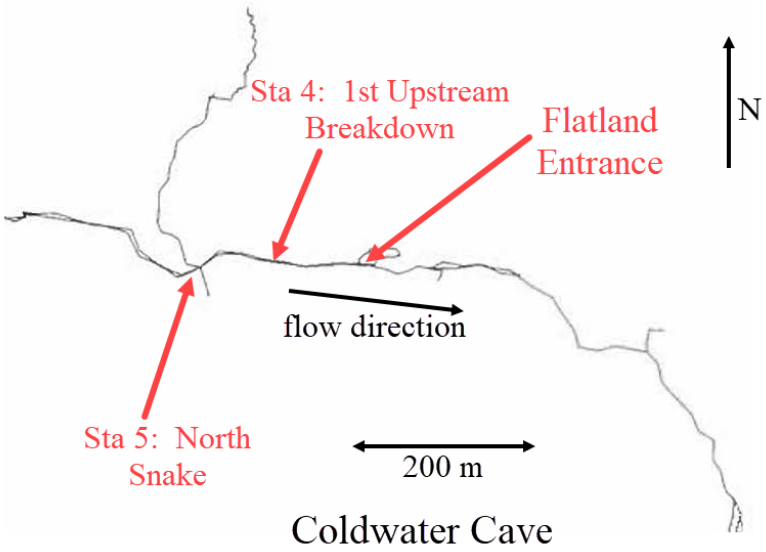

Figure (4): Plan view map of a portion of Coldwater Cave, showing locations of the sampling sites.

locations of sampling sites 4 (1st Upstream Breakdown) and 5 (North Snake). Both of these sites have copious cave sediment, speleothems, and water present in addition to the cave bedrock.

Kemling Cave is the second of the study caves; see Figure (5). It is a shallow mainly horizontal maze cave that has been surveyed to a length of 3.51 km and depth of 21.2 meters. Kemling can be classified as a single entrance cave. The entrance is gated in a manner that permits free air exchange with the outside environment. The locations of the two sampling sites K5 and K34 can be seen in Figure (5). Both of these positions have floors mainly consisting of sediment, with no significant perennial water nearby.

Wonder Cave is the final study cave; see Figure (6). Wonder is an ex-commercial cave that features a drainage watercourse that has a large amount of vertical development from the entrance to a terminal sump more than 44 meters below, and it has a total surveyed length of 0.29 km. Wonder can be classified as a double entrance cave. In addition to the enlarged natural entrance, a second entrance was added during the development of a prior commercial cave tour route to permit transport of construction materials for trail building. The two entrances are at the far ends of the largely linear watercourse, both are gated in a manner that permits free air

exchange with the environment, and the sampling sites W1 and W2 are located in between the two entrances.

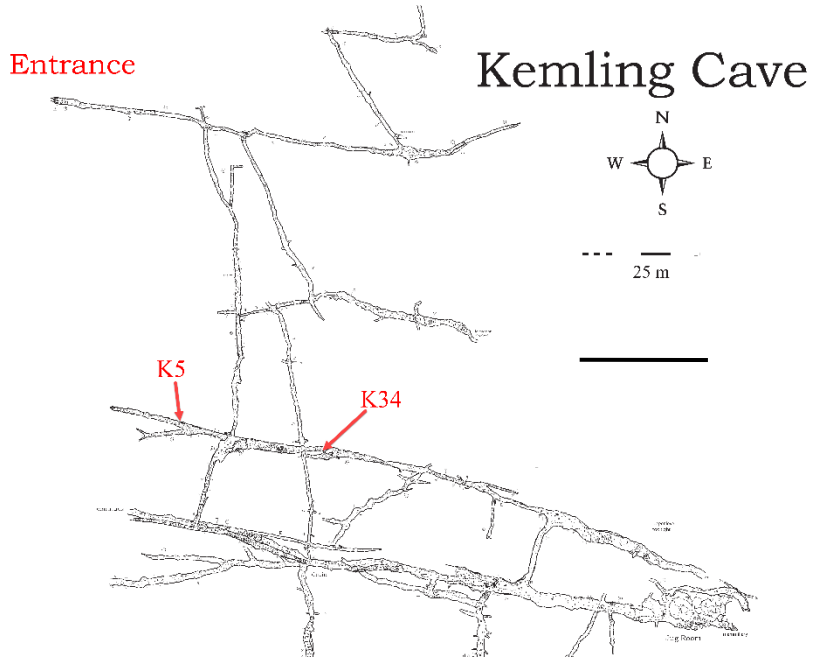

Figure (5): Plan view map of a portion of Kemling Cave, showing locations of the sampling sites.

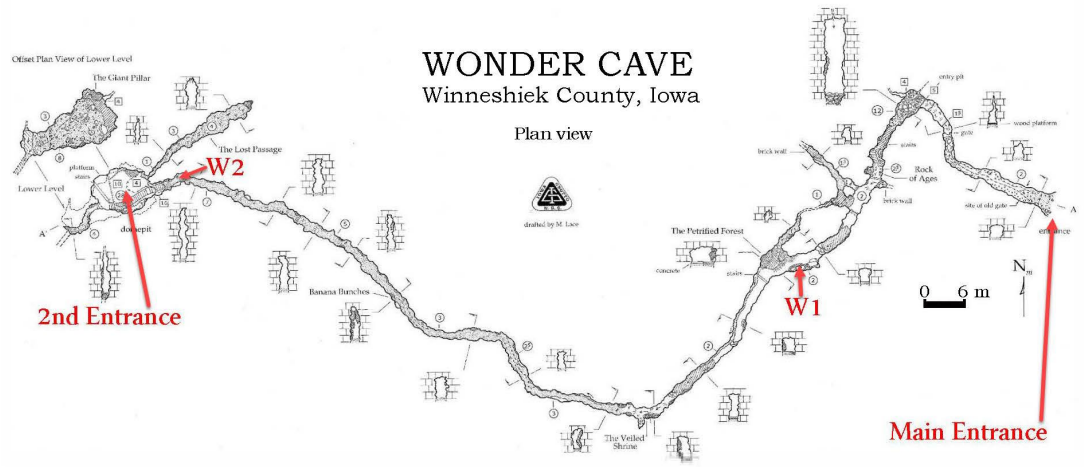

Figure (6): Plan view map of Wonder Cave, showing sampling sites.

Materials and Methods

Integrated average radon activity levels were measured with E-PERM® EIC (Electret Ionization Chamber) sensors, consisting of an electret of either the short-term [ST] or long-term [LT] variety, and a chamber of either the S, or L-OO variety, all from Rad Elec Inc. Chamber volumes were 210, and 58 ml respectively, with the E-PERM becoming more sensitive with an increase in chamber volume. Electret voltages were measured with a SPER-1E electret voltage reader (Rad Elec). Calculations were done with WinSper software Version 2.3.21 or with Radon Report Manager software Version 3.8.44 from Rad Elec. Background gamma radiation exposure was evaluated with the Model 2 Gamma Ray Dosimeter manipulated with the Model 909B charger from Arrow-Tech. The EIC units were deployed in Tyvek® envelopes to protect them from mud and water while in the cave.

Measurements of radon in water were done with the Rad Elec Radon in Water Kit version 2.321. Samples were collected in 68-ml glass bottles featuring Teflon gaskets which were then transferred to a 3.72-L glass measurement jar and evaluated for radon using E-PERMs with ST electrets and S chambers.

Temporal measurements of radon activity were undertaken using Radon Recon® CRM (Continuous Radon Monitor) sensors and Recon Download Tool software v0.9.7 (Rad Elec Inc.) or with Radon Scout Plus CRM sensors and Radon Vision software (Rad Elec). Recon measurements were acquired at 10-minute increments rather than the standard 1-hour increment via spreadsheet manipulation of the raw data file. Both Recon and Scout Plus units were deployed in Tyvek envelopes to protect them from sediment, dust, and water while in the cave. Once in the Tyvek, the sensors were packaged in their thermoplastic cases for transport and deployment in the cave. Prior work demonstrated that both the envelopes and the thermoplastic cases were transparent to radon (Stieff, 2012 and Welch, 2015) and did not impact measured levels.

To minimize the impact of human visitation on the cave atmosphere in Coldwater Cave, the entrance was sealed immediately after human entry and exit, and kept closed throughout the experimental trials. Since Kemling Cave and Wonder Cave were naturally open to the outside atmosphere, there was no need for special airflow protocol during their visitation.

Elemental analysis was performed by Eurofins TestAmerica, St. Louis, using Inductively Coupled Plasma / Mass Spectrometry (ICP/MS). For sediment samples, the elemental concentrations given are for the dry fraction of the sample only. Rock and speleothem samples were cleaned between collection and analysis to minimize contamination with sediment.

Results and Discussion

Elemental analysis results are presented in Table 1, along with earth's crust averages for comparison. As expected, low bedrock uranium was found in the cave samples, with all cave uranium concentrations found to be below 1 ppm and a set median of 0.52 ppm calculated, much lower than the average for the earth's crust. The Wonder Cave samples yielded lower uranium levels than the other two caves, with the exception of the Kemling K5 sample that had no detectable signal for uranium. Although the relative difference in these values was high, there was not an expectation that the concentration of an impurity in the calcium carbonate strata would be highly uniform at different locations. Thorium levels were always slightly higher than uranium, with a set median of 0.87 ppm and the Kemling K5 sample again showing no detectable signal. Set variability for the level of thorium impurities was not unlike that seen for uranium. The slight increase in thorium as compared to uranium reflects the increase seen for the earth's crust average values, although the limestone appears to be even more deficient in thorium than in uranium comparatively. None of the bedrock elemental analyses outcomes would in any way point toward an environment with greatly elevated airborne radon.

The cave sediment uranium concentration seen in Table 1 yielded a more homogeneous data set that produced a median value that was close to that observed for bedrock uranium. However, cave sediment thorium was much higher than bedrock thorium for all samples, with a set median of 4.7 ppm, more than 5 times higher than the bedrock thorium set median. This suggested that the sediment was not derived from the proximate bedrock, but rather had been carried into the cave and away from its genesis location via erosional processes. Subsequent collection of topsoil samples from above all three of the study caves was done, and elemental analysis results in Table 1 showed that the cave sediment thorium was considerably more similar to the topsoil than the cave bedrock, consistent with the erosion hypothesis. All three study caves have active drainage, are wet, and have a history of flooding, so it is not a stretch to envision large inputs of sediment into the cave from external sources. It should be noted that although the sediment samples feature considerably more thorium than the cave bedrock samples, the sediment sample thorium levels are still well below the earth's crust average.

Formation of the calcite speleothems is an example of a recrystallization procedure, where a solid is dissolved into solution and then reprecipitated in solid form. Recrystallizations are a common laboratory procedure for purification of solids, as the crystal lattice of the solid has inherent self-purification properties, requiring foreign ions to fit properly into the crystal lattice of the bulk material. The calcite speleothem uranium levels seen in Table 1 are similar to those seen in both the cave bedrock and sediment samples, whereas three of the four speleothem samples featured undetectable thorium and the fourth a low concentration. This suggests that the recrystallization of the calcite is fairly successful at removing the thorium impurities, but not

the uranium. For the impurities to be conserved in the sample, they need to be soluble in the acidic water that dissolves the bedrock limestone and later serves as the mother liquor for the

Table 1: Elemental analysis data from the study caves. ND = not detectable. Minimum detectable level for solid samples ca. 0.04 ppm for U and 0.08 ppm for Th, for liquids 0.0004 ppm U and 0.0008 ppm Th.

Elemental Analysis Data	Sample	Bedrock U (ppm)	Bedrock Th (ppm)	Sediment U (ppm)	Sediment Th (ppm)	Speleothem U (ppm)	Speleothem Th (ppm)	Water U (ppm)
	Site							
Kemling Cave								
	K34	0.95	1.0	0.82	5.5	0.85	0.34	
	K5	ND	ND	0.59	3.4	0.89	ND	
	Surface			0.92	4.9			
Coldwater Cave								
	4	0.67	0.74	0.53	6.6	0.16	ND	0.00050
	5	0.82	1.3	0.63	7.9	0.61	ND	0.00051
	Surface			0.71	3.2			
Wonder Cave								
	W1	0.36	1.3	0.48	3.6			0.00046
	W2	0.31	0.39	0.60	3.8			
	Surface			0.57	2.3			
Median Cave		0.52	0.87	0.60	4.7	0.73		0.00050
Median Surface				0.71	3.2			

calcite recrystallization. Thorium compounds tend to be insoluble in water, whereas uranium is in general more soluble, making it more available for intercalation into the new crystal (Zhao, 2014). In addition, the released thorium would be expected to form Th^{4+} and the uranium dissolved in acid is likely to form UO_2^{2+} upon dissolution. An impurity ion with a +2 charge would be a better candidate to fill a Ca^{2+} site in a growing crystal lattice than a +4 ion, and thus harder to eliminate in the recrystallization process. Evaluation of the Table 1 data from water samples collected at three of the six stations showed small, but measurable, uranium levels yet undetectable thorium for all. Although these water sources weren't necessarily recrystallizing calcite during the time frame sampled, these data are at least consistent with the notion of the uranium being more soluble than the thorium, and thus more apt to be available for inclusion in recrystallized calcite.

The three stations where water samples were collected for evaluation (results shown in Table 1) all feature perennial flowing streams within the cross section of the sampling site. The other three sites at times feature puddles on the floor or even flowing water during flood conditions, but were dry at the time of data collection. To dovetail with the uranium/thorium analysis of the water from these sites, the concentration of radon dissolved in the water at these stations was measured and the values presented in Table 2. The general rule of thumb for radon in water is that 10,000 pCi/L of dissolved radon will produce 1 pCi/L of radon in the adjacent air (National Research Council, 1999). As such, the radon concentrations in Table 2 represent quite small values.

Table 2: Radon in water measurements for study caves. NA = not applicable

Radon in Water	Sample Site	Dissolved Radon (pCi/L)
Coldwater Cave		
	4	154.5
	5	233.5
Kemling Cave		
	K34	NA
	K5	NA
Wonder Cave		
	W1	42.1
	W2	NA

Radon can concentrate to quite high and problematic values in water, but this typically only happens in completely water-filled spaces underground. When water is in contact with a significant volume of air, the equilibrium constant deems that the radon prefers to outgas from the water into the air (Welch, 1994). Since all three measurement sites feature flowing water that had ample prior exposure to cave airspace upstream of the site, the low dissolved radon readings are not a surprise.

Although radon concentration measurements were made concurrently with sample collection for elemental analysis, it was known that the radon level was variable as a function of time. Since these six sample sites had been commonly used for previous radon measurements, a compilation of all radon measurements made at each site over the prior nine years looked to be a better

yardstick for assessing radon levels than a single trial at each station (Table 3). These data were measured using either CRM and EIC sensors at various times of year. Logistical concerns biased the seasons of data collection away from the winter months. Given the low uranium and thorium levels observed at all these stations, one might expect to see low radon levels in response. The high radon concentration measured in Kemling Cave and the extremely high concentration measured in Coldwater Cave do not follow this logic train. That high radon concentrations are consistently measured in these two caves suggests that these levels are due to lack of ventilation of the caves permitting radon accumulation within the passage. Notably, the radon levels are inversely proportional to the number of cave entrances. Wonder Cave has two entrances straddling the two sample locations. One would expect flow of air between the entrances via the chimney effect, which would keep the radon from concentrating to high levels in this cave and in general produce low within-trial variation of radon concentration.

Table 3: Radon concentration at elemental analysis sites.

Radon Concentration at Elemental Analysis Sites	# of Entrances	Sample Site	Radon # trials	Radon Σ hours	Time Weighted Avg Rn (pCi/L)	Std Dev of set means (pCi/L)	Avg of Within-trial Rn RSD (%)
Coldwater Cave	**0**						
		4	9	277	508.6	166.6	4.4
		5	9	278	494.0	173.2	4.5
Kemling Cave	**1**						
		K34	6	242	210.0	146.5	81.3
		K5	15	596	205.5	160.7	64.9
Wonder Cave	**2**						
		W1	2	110	33.1	3.0	23.0

The low radon concentrations lead to only a small variability from trial-to-trial as well. Kemling Cave has a single entrance, which leads to the cave inhaling and exhaling at the entrance depending on the weather. This produces highly variable radon levels from trial to trial and also within trials, yet the average radon concentration is still high, illustrating that notwithstanding the breathing of the cave, it is still able to accumulate significant amounts of radon despite not having large amounts of the source elements present. Coldwater Cave has very little air movement except for that induced by flowing water. The radon concentrates to very high levels in the cave, and the within-trial relative standard deviation illustrates that the response tends to

be relatively constant throughout a trial. There are long-term changes in radon concentration as can be seen from the standard deviations of the set means, but they tend to happen slowly relative to the time frame of the experiments in this study (times ranging from 14 to 166 hours).

Given the four structural components of the study caves, it appears that the cave water has only a minimal contribution to the airborne radon in the cave. The bedrock, sediment, and speleothems have similar uranium levels and will produce ^{222}Rn at similar rates. The speleothems have almost no thorium, and the sediment has elevated thorium compared to the bedrock values. The relative activity of the differing radon isotopes in the study caves was not determined, but if ^{220}Rn plays a significant role in the underground atmosphere, it is likely originating from the cave sediment. It is postulated that poor ventilation allowing radon to accumulate is a more important factor in these caves than the amount of the parent elements in the vicinity. This would suggest that ^{220}Rn would not be a major player, as its short half-life of 55.6 seconds, compared to 3.823 days for ^{222}Rn (Rumble, 2018), would limit the amount of accumulation that could take place (Kotrappa, 2014).

Acknowledgements

This study would not have been possible without the generous access privileges granted by the landowners of the study caves. Knox College provided financial support to enable this research. Cave map material and survey statistics courtesy of Lawrence Welch, Edward Klausner and Michael Lace. Experimental and theoretical assistance was provided by Jim Roberts, Miah Herrman, Zach Herrman, Beth Welch, and Chris Poe. Photo provided by Scott Dankof.

References

Ayotte, J.D., Flanagan, S.M., and Morrow, W.S., 2007. Occurrence of Uranium and ^{222}Radon in Glacial and Bedrock Aquifers in the Northern United States, 1993-2003. U.S. Geological Survey Scientific Investigations Report 2007-5037.

Cothern, C. R., and Smith Jr., J. E., eds., 1987. Environmental Radon. Plenum Press, New York, p. 82.

El-Taher, A., and Abdelhalim, M.A., 2014. Elemental Analysis of Limestone by Instrumental Neutron Activation Analysis. J. Radioanal. Nucl. Chem., 299, 1949-1953.

Fijałkowska-Lichma, L., 2016. Extremely High Radon Activity Concentration in Two Adits of the Abandoned Uranium Mine 'Podgórze' in Kowary (Sudety Mts., Poland). J. Environ. Radioact., 165, 13-23.

Guilinger, R.R., and Theobald, P.K., 1957. Uranium Deposits in Oolitic Limestone near Mayoworth, Johnson County, Wyoming. U.S. Geological Survey Bulletin 1030-K. 335-342.

Kamaluddin, B., and Amin, Y.M., 1992. Determination of Uranium and Thorium Concentrations in some West Malaysian Limestones using Neutron Activation and Delayed Neutron Analysis. J. Radioanal. Nucl. Chem. Letters, 164(2), 131-135.

Kotrappa, P., Stieff, L., and Stieff, F., 2014. Attenuation of Thoron (Rn^{220}) in Tyvek® Membranes. Proceedings of the 2014 International Radon Symposium, pp. 74-82. http://aarst-nrpp.com/proceedings/2014/12_Kotrappa_ATTENUATION_OF_THORON_Rn220_IN_TYVEK_MEMBRANES.pdf .

Lace, M.J., Kambesis, P.N. and Anderson, R.R., 2021. Iowa Caves and Karst. In: Brick, G. and Alexander, E.C. (eds) *Caves and Karst of the Upper Midwest, USA*. Caves and Karst Systems of the World Series. Springer, Dordrecht.

National Research Council, 1999. Risk Assessment of Radon in Drinking Water. The National Academies Press, Washington DC. https://doi.org/10.17226/6287.

Palmer, A.N., 2007. Cave Geology. Cave Books, Dayton, OH.

Reimer, G.M., and Szarzi, S.L., 2005. Indoor Radon Risk Potential of Hawaii. Journal of Radioanalytical and Nuclear Chemistry, 264(2), 365-369.

Rumble, J.R., Editor-in-Chief, 2018. CRC Handbook of Chemistry and Physics, 99th edition. CRC Press, Boca Raton, 14-17.

Stieff, A., Kotrappa, P., and Stieff, F., 2012. The Use of Barrier Bags with Radon Detectors. Proceedings of the 2012 International Radon Symposium, pp. 67-79. http://aarst-nrpp.com/proceedings/2012/04_THE_USE_OF_BARRIER_BAGS_WITH_RADON_DETECTORS.pdf.

Welch, L.E., and Mossman, D.M., 1994. An Environmental Chemistry Experiment: The Determination of Radon Levels in Water. J. Chem. Educ., 71(6), 521.

Welch, L.E., Paul, B.E., and Jones, M.D., 2015. Measurement of Radon Levels in Caves: Logistical Hurdles and Solutions. Proceedings of the 2015 International Radon Symposium, pp. 1-17. http://aarst-nrpp.com/proceedings/2015/MEASUREMENT_OF_RADON LEVELS_IN_CAVES LOGISTICAL_HURDLES_AND_SOLUTIONS.pdf.

Welch, L.E., Paul, B.E., and Jones, M.D., 2016. Use of Electret Ionization Chambers to Measure Radon in Caves. Proceedings of the 2016 International Radon Symposium, pp. 1-18. http://aarst-nrpp.com/proceedings/2016/Welch_USE_OF_ELECTRET IONIZATION_CHAMBERS_TO_MEASURE_RADON_IN_CAVES.pdf.

Welch, L.E., Paul, B.E., Miller, E.C., Chen, Y.I., Jones, M.D., and Beck, C.L., 2017. Depth Profiling of Radon in Vertical Shafts Using Electret Ionization Chambers. Proceedings of the 2017 International Radon Symposium, pp. 1-18. http://http://aarst-nrpp.com/proceedings/2017/DEPTH-PROFILING-OF-RADON-IN-VERTICAL-SHAFTS-USING-ELECTRET-IONIZATION-CHAMBERS-WELCH.pdf.

Welch, L.E., Takashima, A., Miguel, M.B., Layug, B.C., Jones, M.D., and Beck, C.L, 2018. Correlating Environmental Variables with Radon Activity in an Iowa Cave. Proceedings of the 2018 International Radon Symposium, pp. 1-20. http://aarst-nrpp.com/proceedings/2018/Welch-CORRELATING-ENVIRONMENTAL-VARIABLES-WITH-RADON-ACTIVITY-IN-AN-IOWA-CAVE-2018.pdf.

Welch, L.E., Chen, Y.I, Jones, M.D., and Beck, C.L., 2019. Correlating Radon Activity with Carbon Dioxide Concentration in an Iowa Cave. Proceedings of the 2019 International Radon Symposium. https://aarst.org/proceedings/2019/CORRELATING-RADON-ACTIVITY-WITH-CARBON-DIOXIDE-CONCENTRATION-IN-IOWA-CAVE-WELCH-2019.pdf.

Zhao, M., and Zheng, Y., 2014. Marine Carbonate Records of Terrigenous Input into Paleotethyan seawater: Geochemical constraints from Carboniferous limestones. Geochimica et Cosmochimica Acta, 141, 508-531.